ANALYSIS OF LCLS-SC COMMISSIONING AND OPERATIONAL QUENCHES*

N. R. Neveu†, S. Aderhold, L. E. Alsberg, L. Alston, D. Gonnella, J. T. Maniscalco,
H. A. Marts, J. Nelson, R. D. Porter, L. Zacarias
SLAC National Accelerator Laboratory, Menlo Park, CA, United States

Abstract

LCLS-SC achieved first light in 2023 and continues to ramp up performance. The linac consists of 35 cryomodules at 1.3 GHz, plus two cryomodules operating at the 3rd harmonic (3.9 GHz). The high repetition rate linac has been operating at 3.8 GeV regularly since 2024. As with any SRF machine, quenches occurred both during commissioning (as a part of normal processing) and during normal operations (tuning and beam delivery). After several years of operation, there are now thousands of quench events that can be analyzed and mapped to machine performance. In this work, quench rates in all cavities in the linac are identified and compared to operational quench rates and gradient limits.

INTRODUCTION

The Linac Coherent Light Source facility consists of two linear electron linacs, one normal conducting (NC) and one superconducting (SC) both installed in the existing SLAC 3 km tunnel. The NC linac, now called LCLS-NC, has been operating as a Free Electron Laser (FEL) since 2009. An upgrade of the facility (LCLS-II) installed an SC linac in the first third of the tunnel. The SC linac, now called LCLS-SC, is the first superconducting accelerator operated at SLAC. LCLS-SC has been commissioned and operated from 2022 to 2025. First light was accomplished in August 2023, and through 2025 regular user delivery and machine development took place. Simultaneous delivery to both hard and soft x-ray hutches was demonstrated in preparation for the increase in beam energy from the LCLS-II-HE project. Starting in December 2025, LCLS-SC was shut down for planned construction of LCLS-II-HE, another upgrade project that will add an additional 23 cryomodules to the LCLS-SC linac (L4). This will increase the operational energy from 4 GeV to 8 GeV starting in 2027. After the new cryomodules are commiossitoned, the repetition rate will ramp-up to 1 MHz. See Fig. 1 for the full LCLS-SC layout that includes both LCLS-II and LCLS-II-HE.

Currently, LCLS-SC contains four main accelerating sections: L0, L1, L2, and L3 with a total of 35 cryomodules operating at 1.3 GHz. Each cryomodule contains eight superconducting TESLA-style RF cavities [1] made of niobium. This type of cavity and variations on the cryomodule design are installed in several facilities, including Eu-XFEL and Fermilab. In this work, we review all commissioning and operational quenches during the 2022-2025 run of LCLS-SC. In Section , we review the current quench classification method at SLAC and typical SRF cavity decay and quench waveforms. In Section , we then use the classification method to analyze all historical quenches for LCLS-SC, including false quenches, multipacting processing events, and normal operations.

QUENCH CLASSIFICATIONS

SRF cavity quenches occur when an SC cavity loses SC properties and becomes normal conducting. This can occur due to impurities in the cavity surface during fabrication, installation and/or migration of particles during operation [2]. Once a small spot on the cavity surface becomes normal conducting, heat is dissipated throughout the cavity and it is no longer able to hold the operating gradient. These quenches are not as violent as SC magnet quenches, and once the cavity cools down again, it can resume operation. Typically, if caught fast enough, turning off the cavity prevents serious impact to the accelerator, and the cavity can be returned to operation within minutes or less. The quench, cool down and reset pattern is the reason a robust interlock system is needed. If the power supplied to a quenched cavity is not stopped, the cavity will continue to remain normal conducting and cause a disturbance in the helium bath (i.e. becoming a high heat load on the cryogenics system). The LCLS-SC interlock system compares the forward and reverse power supplied to the cavity. Although the heat load issue is a transient problem solved by robust interlocking, there is also the potential for trapped magnetic flux in the cavity after a quench. This is a persistent negative effect of quenches, which reduces the quality factor of the cavity (Q) [2]. Trapped magnetic flux can be purged with a fast cool down of the cavity, but that is not a routine operation. All attempts are made to reduce the number of warm up and cool down cycles necessary for maintenance and operations. Each warm and cool cycle takes 2-3 days, which impacts operational up time and delivery to users.

With high heat load being the high impact effect of quenches, the interlock detection is intentionally conservative. It often results in 'false' quenches: events flagged as a quench, but in which the cavity turns off for another reason. During normal operations, an SRF cavity might shut off for a variety of reasons, including tunnel access, equipment health, or beam tuning in targeted areas. When the interlock sees this drop in power, it is logged as a quench. To reduce the number of quench waveforms flagged for human review, a classification function and watcher process were written to reset LCLS-SC cavities when the quench is false. This is

* Work supported by the U.S. Department of Energy under contract DE-AC02-76SF00515.
† nneveu@slac.stanford.edu

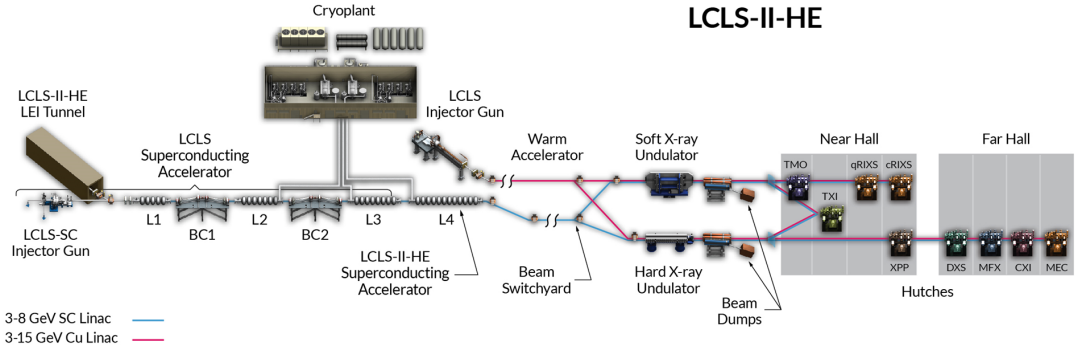

Figure 1: LCLS-SC facility layout. L4 is currently being installed under the LCLS-II-HE project, with commissioning expected in 2027.

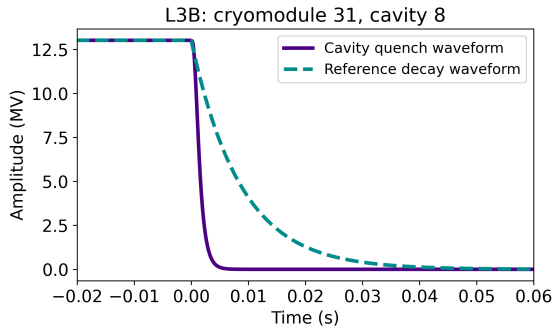

Figure 2: Real quench and normal decay waveforms. Data taken from cryomodule 31, cavity 8 in L3.

done by looking at the decay waveform saved after the interlock is triggered. An example of a quench decay (steep drop) and normal decay is shown in Fig.2. Each time an interlock is triggered, a waveform like the ones in Fig. 2 is saved to a text file and process variable (PV) for classification.

The current classification method fits the cavity waveform data, calculates the loaded Q-value (Q_L), and uses Q_L to determine if a quench is real or false. This classification method has three main steps: (1) trimming the data to focus only on the cavity decay, (2) linearization and fitting of the decay, and (3) comparing the stored Q-value for that cavity (Q_s) to the newly calculated Q_L. In (3) a threshold is used to determine if the newly calculated Q_L is labeled real or false.

For step (2), an exponential form can be assumed for the amplitude of a normal cavity decay [2]:

$$A(t) = A_0 \cdot e^{-\frac{\pi f t}{Q_L}} \tag{1}$$

where A_0 is the pre-quench amplitude (first value of the fault amplitude array), f is the frequency, t is time, and Q_L is the loaded Q-value for the quench. Equation 1 is then linearized to isolate Q_L. The natural log is used to simplify as follows:

$$ln\left(\frac{A_0}{A(t)}\right) = \frac{\pi f t}{Q_L} \tag{2}$$

The third and final step in the classification method is used to calculate and compare the Q-values. In order to calculate Q_L the equation for the slope is rearranged. For notation purposes, 'exponential_term' is referred to below as 'x_e' and refers to the slope calculated when the exponential form of the decay was linearized. We can now solve for Q_L:

$$Q_L = \frac{\pi f}{x_e} \tag{3}$$

Then, to calculate the threshold, which is the minimum acceptable Q_L before a quench is considered real, the saved Q_s extracted from the quench file is multiplied by 0.6, for a threshold of 60%. Cavities that have interlock quench events flagged as false are quietly reset and turned back on automatically with a watcher process. Quenches that are classified as real require a human in the loop to reset and try to determine the cause of the quench and mitigation options.

OPERATIONAL QUENCH DATA

With the current classification method, we can review all commissioning and operational quench data for LCLS-SC from 2022-2025. A total of 105,481 quench interlock events were recorded, with 65.5% of those being false see Fig. 3. From this result we can confirm empirically the interlock threshold is sufficiently conservative. For further analysis false quench events were filtered out of the dataset and high count outliers (i.e. CM20/34/35) were investigated. The cryomodules with elevated quench levels compared to the machine average had multipacting (MP) processing on one or more occasions. MP processing is done before a fast cool down as time allows. The process is similar to processing in NC cavities. Electrons are emitted from the surface of the cavity and can cause secondary emission of elections. This limits the maximum operating gradient of the cavity and is typically accompanied by a short burst of radiation and/or a quench. MP processing is not performed during normal operations, as it requires changing the cavity gradient and can disrupt beam operations. When possible, MP processing is scheduled before a fast cool down, so that any trapped magnetic flux can be purged. In the case of the outliers CM34 and CM35, both had RF pulsed processing applied. Instead of operating CW, short RF pulses are applied in rapid succession with the goal of disrupting the conditions at field emitting sites in the cavity. This has been shown to increase the usable gradient due to field emission in cavities at several facilities [3].

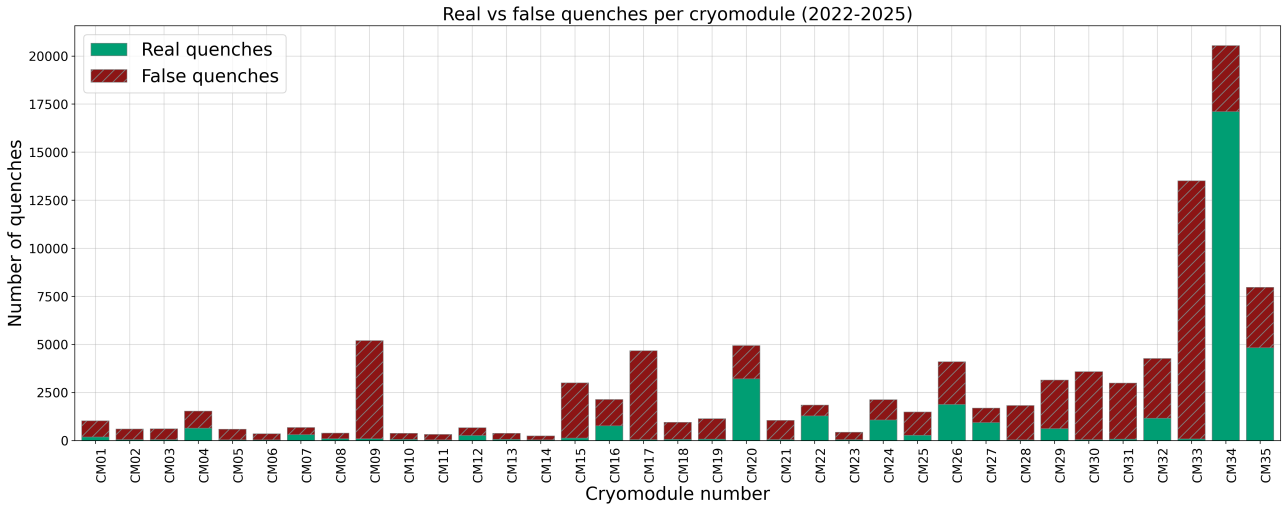

Figure 3: Percentage of real and false quenches over the 2022-2025 period.

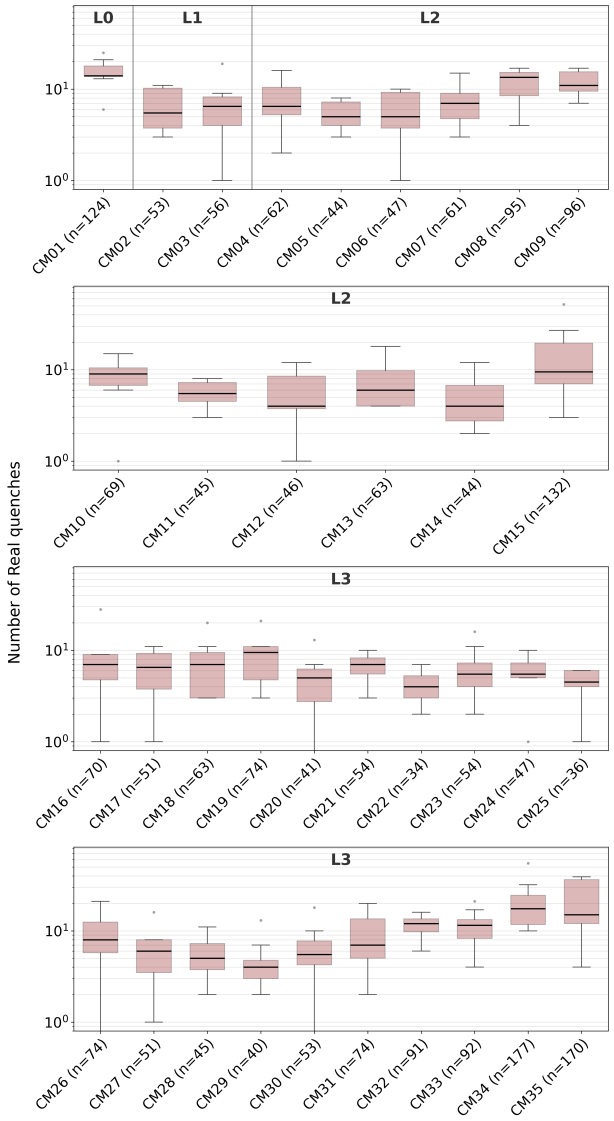

Figure 4: Distribution of quench events in each cavity. Only real quenches are shown here, false events and multipacting processing days are filtered out.

Next, to distinguish between intentional and unintentional quench events, all processing events were filtered out. The resulting data should then be a fair representation of operational quench rates in LCLS-SC. Fig. 4 shows a box plot of the remaining quench distributions across each cryomodule after filtering out false and processing events. Each box in the plot represents data for 8 cavities (1 cryomodule). The box starts at quartile 1 and extends to quartile 3, which is called the interquartile range (IQR). The line in the box marks the median and the whiskers extend 1.5x of the IQR [4]. From these data, we can confirm that the average quench rate per cavity per day is below one. Some cavities have not quenched or have only quenched very rarely (whiskers near zero). This conclusively indicates the LCLS-SC linac is operating stably with very low quench rates.

CONCLUSION

LCLS-SC has been operating successfully from 2022 to 2025. The current quench interlock and classification methods are sufficiently conservative to protect the machine, with 65.5 % of quench interlock events being false quenches. The majority of real quench events are intentional multipacting or pulsed processing. The real quench rates during machine development or user delivery (nominal operations) are very low. LCLS-SC records less than one quench per cavity per day on average. Future work will focus on improving classification methods and quench detection to reduce the number of false positives. Efforts will be made to learn from other ongoing works in the community [5–9]

ACKNOWLEDGMENTS

This work used the resources of the SLAC Shared Science Data Facility (S3DF) at SLAC National Accelerator Laboratory. S3DF is a shared High-Performance Computing facility, operated by SLAC, that supports the scientific and data-intensive computing needs of all experimental facilities and programs of the SLAC National Accelerator Laboratory. SLAC is operated by Stanford University for the U.S.

Department of Energy's Office of Science. This work was funded under DOE Contract No. DE-AC02-76SF00515.

REFERENCES

[1] B. Aune *et al.*, "Superconducting tesla cavities", *Physical Review Special Topics - Accelerators and Beams*, vol. 3, no. 9, 2000. doi:10.1103/physrevstab.3.092001

[2] H. Padamsee, J. Knobloch, and T. Hays, *RF Superconductivity for Accelerators*. Wiley, 1998. http://books.google.com/books?id=2leaQgAACAAJ

[3] "TTC collaboration meetings", 2024, https://tesla.desy.de/meetings/collaboration_meetings_and_ttc_workshos/,

[4] "Matplotlib documentation", 2026, https://matplotlib.org/stable/api/_as_gen/matplotlib.pyplot.boxplot.html,

[5] L. Boukela, J. Branlard, and A. Eichler, "Exploring nas for anomaly detection in superconducting cavities of particle accelerators", *Frontiers in Physics*, vol. 13, May 2025. doi:10.3389/fphy.2025.1553993

[6] A. Bellandi *et al.*, "Online detuning computation and quench detection for superconducting resonators", *IEEE Transactions on Nuclear Science*, vol. 68, no. 4, pp. 385–393, Apr. 2021. doi:10.1109/tns.2021.3067598

[7] A. Eichler *et al.*, "Enhancing quench detection in SRF cavities at the EuXFEL: Towards machine learning approaches and practical challenges", in *Proc. IPAC'25*, Taipei, Taiwan, pp. 3226–3229, Nov. 2025. doi:10.18429/JACoW-IPAC2025-THPS134

[8] G. Martino *et al.*, "Anomaly Detection Based Quench Detection System for CW Operation of SRF Cavities", no. 31, pp. 775–777, Oct. 2022. doi:10.18429/JACoW-LINAC2022-THPOPA15

[9] M. M. Rahman, A. Carpenter, K. Iftekharuddin, and C. Tennant, "Accelerating cavity fault prediction using deep learning at jefferson laboratory", *Machine Learning: Science and Technology*, vol. 5, no. 3, p. 035078, 2024. doi:10.1088/2632-2153/ad7ad6